DENTAL MATERIALS 35 (2019) e272–e285

Available online at www.sciencedirect.com

ScienceDirect

journal homepage: www.intl.elsevierhealth.com/journals/dema

Improved mechanical performance of self-adhesive resin cement filled with hybrid nanofibers-embedded with niobium pentoxide

Marilia M.A.C. Velo[a,*], *Tatiana R.L. Nascimento*[c,d], *Cassiana K. Scotti*[a], *Juliana F.S. Bombonatti*[a], *Adilson Y. Furuse*[a], *Vinícius D. Silva*[c], *Thiago A. Simões*[c], *Eliton S. Medeiros*[c], *Jonny J. Blaker*[d], *Nikolaos Silikas*[b], *Rafael F.L. Mondelli*[a]

[a] *Bauru School of Dentistry, University of São Paulo-USP, Bauru, SP, Brazil*
[b] *Dentistry, School of Medical Sciences, The University of Manchester, Manchester M13 9PL, UK*
[c] *Materials and Biosystems Laboratory (LAMAB), Department of Materials Engineering (DEMat), Federal University of Paraíba (UFPB), João Pessoa, Brazil*
[d] *Bio-Active Materials Group, Department of Materials, MSS Tower, The University of Manchester, Manchester, M13 9PL, UK*

ARTICLE INFO

Keywords:
Cotton-wool-like nanofibers
Hybrids
Mechanical properties
Niobium pentoxide
Resin cement
Solution blow spinning

ABSTRACT

Objectives. In this study hybrid nanofibers embedded with niobium pentoxide (Nb_2O_5) were synthesized, incorporated in self-adhesive resin cement, and their influence on physical-properties was evaluated.

Methods. Poly(D,L-lactide), PDLLA cotton-wool-like nanofibers with and without silica-based sol–gel precursors were formulated and spun into submicron fibers via solution blow spinning, a rapid fiber forming technology. The morphology, chemical composition and thermal properties of the spun fibers were characterized by field emission scanning electron microscopy (FE-SEM), energy dispersive X-ray spectroscopy (EDS) and Fourier-transform infrared spectroscopy (FTIR), and differential scanning calorimetry (DSC), respectively. Produced fibers were combined with a self-adhesive resin cement (RelyX U200, 3 M ESPE) in four formulations: (1) U200 resin cement (control); (2) U200 + 1 wt.% PDLLA fibers; (3) U200 + 1 wt.% Nb_2O_5-filled PDLLA composite fibers and (4) U200 + 1 wt.% Nb_2O_5/SiO_2-filled PDLLA inorganic–organic hybrid fibers. Physical properties were assessed in flexure by 3-point bending ($n = 10$), Knoop microhardness ($n = 5$) and degree of conversion ($n = 3$). Data were analyzed with One-way ANOVA and Tukey's HSD ($\alpha = 5\%$).

Results. Composite fibers formed of PDLLA-Nb_2O_5 exhibited an average diameter of ~250 nm, and hybrid PDLLA + Nb_2O_5/SiO_2 fibers were slightly larger, ~300 nm in diameter. There were significant differences among formulations for hardness and flexural strength ($p < 0.05$). Degree of conversion of resin cement was not affected for all groups, except for Group 4 ($p < 0.05$).

---

* *Corresponding author at*: Alameda Dr. Octávio Pinheiro Brisolla, 9-75 - Jardim Brasil, Bauru, SP, 17012-901, Brazil.
E-mail address: mariliavelo@usp.br (M. M.A.C. Velo).

https://doi.org/10.1016/j.dental.2019.08.102

Significance. Hybrid reinforcement nanofibers are promising as fillers for dental materials. The self-adhesive resin cement with PDLLA + Nb_2O_5 and PDLLA + Nb_2O_5/SiO_2 presented superior mechanical performance than the control group.

1. Introduction

Improvements in the field of dental materials include a wide range of adhesive resin cements for luting indirect restorations [1]. In part, the clinical success of indirect restorations is ensured by the choice of luting agent and correct execution of the cementation technique to generate a strong bond between the tooth and the restoration [2]. Mechanical properties of resin cements also influence the fracture strength of restored teeth with indirect restorations and therefore, higher flexural strength and hardness values could lead to greater fracture resistance [3].

Self-adhesive resin cements were introduced to simplify cementation procedures as no dental substrate pretreatment is required [4,5]. They have attained great popularity because they simplify adhesive luting procedures, reducing technique sensitivity and chairside time [4]. However, at the same time that the application procedure is simpler, compared with conventional resin cements and no postoperative sensitivity is expected because the smear layer is not removed, they interact only superficially with the dentin substrate resulting in lower bond strength [6,7]. These cements present modified acidic groups containing methacrylate monomers that are able to demineralize and infiltrate the dental substrate, resulting in mechanical retention [4]. In addition, the monomers possibly develop chemical interactions between the resin cement and the Ca^{+2} of hydroxyapatite [4,5]. In the beginning of the chemical reaction, the initially acid pH is neutralized and increases from 1 to 6 to avoid impairing the end conversion of monomers, which could jeopardize the mechanical properties of the cross-linked resin [2]. Meanwhile, the acid monomers react with the amine co-initiator and camphorquinone resulting in lower polymerization rates and reducing the degree of conversion (DC) of monomers, which can negatively influence the clinical performance [8,9]. Therefore, in spite of being extensively used nowadays, the self-adhesive resin cements are still progressing and further mechanical improvements are needed to achieve long-term satisfactory cementation using this class of resin cements.

Some efforts have been made to reinforce resin-based dental materials with nanostructures to achieve enhanced clinical performance [10,12]. Indeed, the incorporation of submicron titanium dioxide, silica or hydroxyapatite-materials has shown promising results on physical-mechanical properties of resin composites [8,12], adhesives [13], glass ionomer cements [14] and resin cements [15,16].

The incorporation of pentoxide niobium (Nb_2O_5) to biomaterials has also been highlighted due to its remarkable physicochemical properties and high biocompatibility showing potential in biomedical applications [17]. Nb_2O_5 is a metal oxide, insoluble in water, with high mechanical stability and similar optical properties to the dental structure [18]. It also presents bioactivity and promotes the growth of hydroxyapatite crystals when in contact with human saliva [19]. In the case of self-adhesive resin cements, it could be hypothesized that the incorporation of Nb_2O_5 nanostructures could be used as reinforcement to improve their mechanical properties. Furthermore, based on the interaction between self-adhesive cements and tooth substrates, the addition of Nb_2O_5 might improve the marginal sealing with restorations and this modified material would be suitable for further researches in a biomimetic remineralization approach.

On the other hand, since the inorganic filler are harder than the organic matrix of resin-based materials, stresses are transmitted onto the filler structures during masticatory forces, which generate cracks around the filler particles [20]. Therefore, reinforcement with fibrous materials have gained interest in dental materials researchers in the past decade [11,21]. Nanofibers are considerably more ductile than inorganic fillers [20] and their extreme reduced diameter results in significant increase in strength [22]. Nanofibers also provide a large ratio of surface area to volume, which can enhance the intermolecular hydrogen bonding between the nanofibrous filler and the resin matrix, providing good load transfer between them [20].

In tissue engineering, sol–gel and sol–gel inorganic–organic hybrids are promising materials for regeneration applications because they can impart bioactivity, act as platforms for therapeutic ion release, and recently self-healing systems have been reported [23,24]. Different configurations include 3D-scaffolds, foams, fiber mats, and cotton-wool-like nanofibers that can even be 3D-printed [25]. Although the current evidence shows positive results related to the incorporation of nanofibers composed of organic polymers in resin composites [21,26], their addition into resin cement should be also investigated. Moreover, the use of inorganic–organic hybrid nanofibers in dental materials field could be explored, since these hybrid fibers can act as a platform for the release of therapeutic ions such as strontium, silver, iron, fluoride and copper [27]. The addition of Nb_2O_5 powder to sol–gel derived nanofiber precursors is expected to improve their mechanical properties and also the DC, as Nb_2O_5 is a semiconductor oxide, presents photocatalytic properties and, therefore, high energy absorption [18,28].

Thus, the aim of this study was to fabricate/synthesize hybrid nanofibers embedded with orthorhombic niobium pentoxide with or without a network on silica (Nb_2O_5/SiO_2) and characterize their morphology and composition. Then, we evaluated the effects of their incorporation on the overall mechanical properties and DC of a self-adhesive resin cement, compared to the self-adhesive resin cement itself and the self-adhesive resin cement filled with organic nanofibers. It was hypothesized that the inclusion of hybrid nanofibers would influence the Knoop microhardness and flexural strength of self-adhesive resin cements. It was also hypothesized that the self-adhesive resin cement would present higher DC values, as Nb_2O_5 presents photocatalytic properties, which improves the light absorbtion near the visible region of the light spectrum.

2. Materials and methods

2.1. *Materials*

A commercial self-adhesive resin cement (RelyX U200, 3 M ESPE) composed of a base (methacrylate monomers containing phosphoric acid groups, initiators, stabilizers and rheological additives) and a catalyst paste (methacrylate monomers, alkaline fillers, silanated fillers, initiator, stabilizers, rheological additives) was used in this study. RelyX U200 was selected due to the reduced viscosity and superior bonding performance to enamel and dentin in comparison with other self-adhesive cements [29,30]. This cement is based on the chemistry of its predecessors RelyX Unicem (the first self-adhesive resin cement introduced in the market) and U100 with the addition of a rheology modifier to the mixture, which reduces the viscosity.

The nanofibers used were composed by Poly(D,L-lactide), PLA 4060D, PDLLA, with an average molecular weight of 120 kg/mol, was obtained from Jamplas Inc., MO, USA, in pellet form. Dimethyl carbonate (DMC > 99%, Sigma–Aldrich, Germany) was used as solvent for PDLLA. Niobium oxide powders (99.9% orthorhombic, Nb_2O_5) was obtained from AMG company, BRA. Tetraethyl orthosilicate (TEOS ≥ 99% purity) was obtained from Sigma–Aldrich, Germany and used as a precursor for the synthesis of silica, inorganic–organic sol–gel. Ethanol (≥99.5% purity) and HCl (1.0 M standard) were purchased from Sigma–Aldrich (United Kingdom).

2.2. *Milling and particle size analysis of Nb2O5 powders*

Niobium oxide powders were milled to reduce and homogenizer their particles size. Wet milling was conducted using a suspension of the niobium oxide powder in ethanol using a conventional mill loaded with zirconia balls (SERVITECH, CT-241, 5 mm in diameter) and rotating at 60 rpm for 1 h. Then, the powder was filtered, dried overnight at 50 °C and stripped for deagglomeration. Particle size was determined by dynamic light scattering (DLS) using a Zetasizer Nano-ZS90 (Malvern Panalytical, USA) with a Nb_2O_5 setup of 0.21 cm^{-1} absorption coefficient and 2.34 refractive index. Dilution for measure was carried out with distilled water using a concentration of 1 wt.%.

2.3. *Organic nanofiber, composite submicron fiber and inorganic–organic hybrid sol–gel -based nanofiber fabrication*

A conventional method of solution blow spinning (SBS) was used to produce the fibers, using a set-up as described in [24,31,32]. In this work the parameters for spinning were: internal (1.6 mm) and external (3 mm) nozzle diameter, 45 psi pressure, flow rate 7.2 mL/h, 2 mm nozzle protrusion, and working distance of 20 cm at 40 °C (the hood remained with controlled temperature). Three-dimensional Poly (D,L-lactide, PDLLA) cotton-wool-like fibers were obtained by a rotating collector at ~19 m/s. Poly (D,L-lactide, PDLLA) cotton-wool-like nanofibers with and without niobium filler or silica-based sol–gel precursors were formulated and spun into submicron fibers via SBS. Composite fibers were produced with precursor solutions of niobium-filled PDLLA fibers.

Inorganic–organic hybrid sol–gel-based fibers were produced with a silica precursor solution A using formulations based on the work of Poologasundarampillai et al. [31], in the stoichiometric ratio of 1:2:2:0.01 (TEOS, ethanol, H_2O and 1 M HCl), respectively in order to hydrolyze TEOS. The solution was prepared under constant stirring for 24 h at room temperature. Separately, a second polymer solution B was prepared (20% in mass) to contain initially 10 wt.% of niobium added (in relation to the total polymer mass) in 10 mL of DMC and sonification was performed for 3 h at 8 min intervals every hour. Next, the mass of PDLLA was added to the initial solution under stirring for 6 h at 80 °C. Subsequently, 3.7 mL of solution A was slowing dripped onto 7.3 mL of solution B (30 wt.% of silica) and constant stirring at room temperature per 3 h to result in the inorganic–organic hybrid solution. Fig. 1 illustrates an overview of the SBS fibers production.

2.4. *Fiber characterization*

Fiber morphology was assessed using a field emission scanning electron microscope (FESEM) coupled with energy dispersive X-ray spectroscopy (EDS), described in [33,34]. Fiber diameters were measured using ImageJ software (version 1.48, NIH, Bethesda, MD, USA), based on a minimum of 70 fibers per each sample.

The thermal properties were assessed using differential scanning calorimetry (DSC) on a DSC 60 (Shimadzu, Japan). Samples were heated from 25 to 200 °C under nitrogen atmosphere (50 ml min^{-1}) at a heating rate 10 °C min^{-1}.

2.5. *Self-adhesive resin cement sample preparation*

The samples were prepared by mixing the fibers (as described above) into the RelyX U200 commercial self-adhesive resin cement. The same portion of base and catalyst pastes was dispensed on a mixing pad and weighted on a precision scale (Denver Instrument, São Paulo, Brazil). Next, 1 wt.% of fibers were weight with the value corresponding to the resin cement mass. This percentage was determined in previous pilot studies varying the fibers concentration in order to obtain a sufficient fluidity cement with improved mechanical properties. Fibers were manually added to the base paste and mixed for 10 s. Afterward, the base paste with fibers were mixed with the catalyst paste for another 10 s, according to the manufacturer instruction. All samples were light-activated according to the manufacturer's instruction with a third generation LED device (Valo, Ultradent) operating at 1000 mW cm^{-2} for 20 s at 1 mm distance. The irradiance was measured as previously described [35].

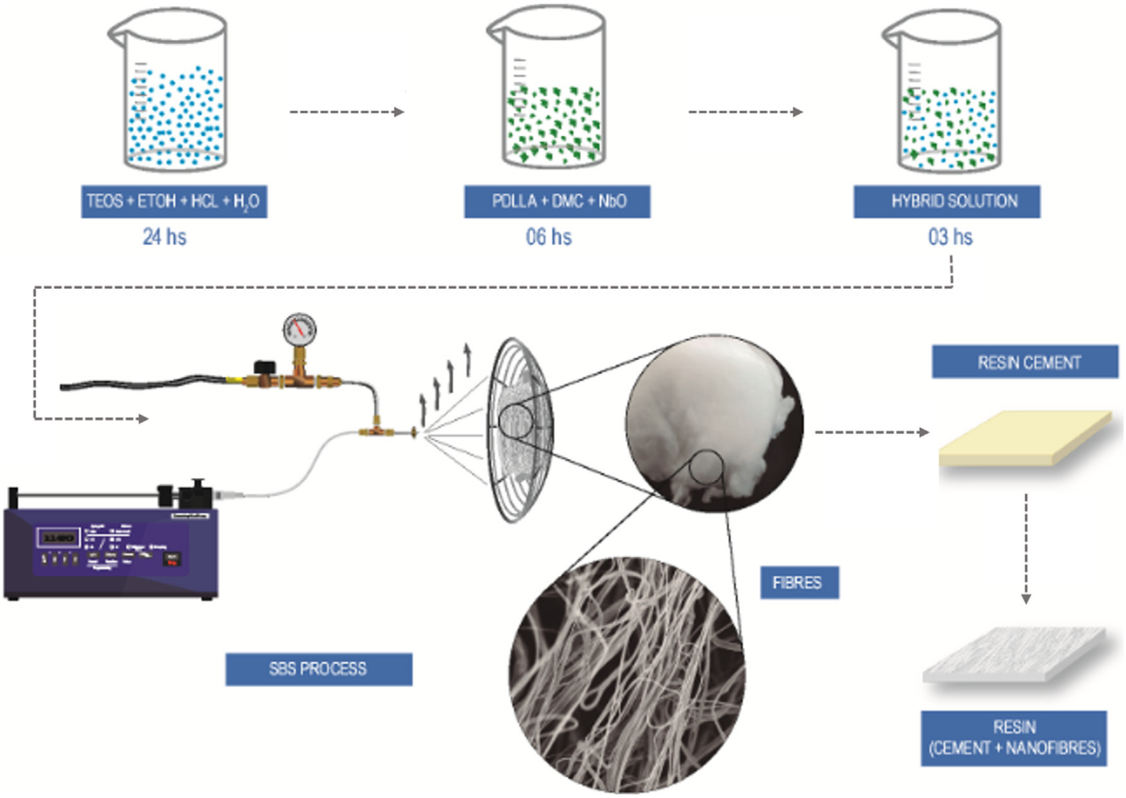

Fig. 1 – Schematic representation of the SBS fibers production.

The groups formed were as follow: (1) U200 resin cement (control); (2) U200 + 1 wt.% PDLLA nanofibers; (3) U200 + 1 wt.% Nb_2O_5-filled PDLLA composite submicron fibers; and (4) U200 + 1 wt.% Nb_2O_5/SiO_2-filled PDLLA inorganic–organic hybrid nanofibers.

2.6. *Flexural bending tests*

Bar-shaped samples measuring 8 mm × 2 mm × 2 mm were prepared by pouring the mixtures described above into stainless-steel split-molds, according to ISO 4049 with modification of the sample length to avoid overexposure or uncured regions considering the diameter of the LED curing device. Five samples were prepared per group.

The flexural evaluation was conducted using a universal testing machine (Instron 5943, Norwood, MA, USA), equipped with a 500 N load-cell, using a crosshead speed of 0.5 mm/min, according to ASTM D 790-86. Samples were loaded in 3-point bending using a 6 mm span length on the top surface of each specimen. Values were determined with the following equation:

$$FS = \frac{3Fl}{2bd2} \qquad (1)$$

Where FS is the flexural strength in MPa; F is the loading force at the fracture point, l is the length of the support span (6 mm), b and d are the measured width and thickness, respectively. Fracture surface was analyzed by scanning electron microscope (SEM).

2.7. *Knoop microhardness determination*

Disc-shaped samples measuring 10 mm in diameter and 2 mm in thickness were prepared by placing the material into stainless-steel molds and covered with a polyester strip. The surface of the samples was polished using decreasing grit abrasive papers (in series 600, 1200, 2400, Buehler Ltd., Lake Bluff, IL, USA) for 2 min each, followed by 0.5 μm diamond paste (Buehler Ltd., Lake Bluff, IL, USA) to obtain flat and smooth surface suitable for hardness evaluation. Three indentations were made on the top surface of each specimen along a middle line spaced 100 μm from each other (Knoop diamond, 50 g, dwell-time 15 s), using a digital microhardness equipment (Micromet II, Buehler, USA) and the mean of the three readings was obtained.

2.8. *Degree of conversion*

The DC was evaluated with FTIR-ATR (FTIR 8400; Shimadzu) with a resolution of 4 cm^{-1} and 32 scans ranging from 4000 to 800 cm^{-1}. Samples (n = 5) were analyzed after mixing the base and catalyst paste under dual-cure polymerization condition. The mixture was immediately placed covering the ATR crystal to obtaining the baseline spectra. This was considered the initial FTIR spectra for the DC calculation. Three minutes after mixing the pastes, the material in the crystal was photo-activated for 20 s and the spectra collection was repeated (Fig. 2).

The percentage of unreacted carbon double bonds (C=C) was obtained from the peak height ratio of the methacrylate

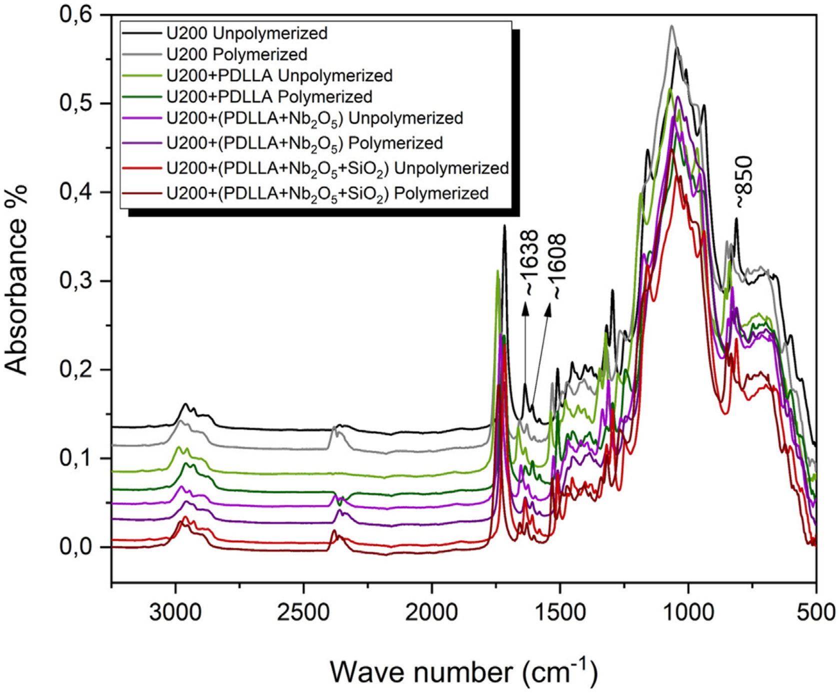

Fig. 2 – Peaks at 1608 and 1638 cm^{-1} identified in the spectral bands used for calculating the degree of conversion immediately after mixing the base and catalyst pastes in a dual-cure polymerization condition and after photo-activation. Peak at 850 cm^{-1} identified the Nb.—O—Si linkage.

C=C (at 1638 cm^{-1}) and those of an internal standard aromatic carbon double bond (at 1608 cm^{-1}) during the polymerization in relation to the uncured material. The percentage of degree of conversion (%DC) was calculated for each sample as follow:

$$DC\,(\%) = \frac{1 - R_{3min}}{R_{baseline}}.100 \qquad (2)$$

where R is the ratio of the absorbance at 1638 cm^{-1} and absorbance 1608 cm^{-1} as a function of time.

2.9. *Statistical analysis*

Kolmogorov-Smirnov normalization test was applied to examine if variables were normally distributed. Flexural strength, Knoop microhardness and DC (quantitative data) were analyzed using one-way ANOVA followed by the Tukey's HSD test. The level of significance was pre-set at $\alpha = 0.05$.

3. Results

3.1. *Fibers morphology*

Niobium pentoxide particles were estimated at approximately 60 ± 10 nm in size by DLS measurement (Fig. 3) and were used in colloidal solution to obtain fibers in inorganic–organic sol–gel. Based on the DLS analysis it was concluded that niobium particles did not agglomerate (Fig. 3). When agglomeration occurs, there are different peaks in smaller and large sizes or duplicates. Typical samples consisted of cotton-wool-like fibers and soft sponge-like structures, as previous described [36,37]. The results showed that PDLLA nanofibers presented diameter of 0.1 ± 0.1 μm (Fig. 4a). Submicron and nanofibers of circular cross-section for Nb_2O_5-filled PDLLA and Nb_2O_5/SiO_2-filled PDLLA presented diameters ranging of 0.25 ± 0.1 μm (Fig. 4b) and 0.3 ± 0.1 μm (Fig. 4c), respectively. Nb_2O_5-filled PDLLA composite fiber samples presented homogeneity, network and porosity among the fibers. Nb_2O_5/SiO_2-filled PDLLA obtained combined fibers, which was attributed to some variations in the pressure and to the inorganic/organic precursor ratio.

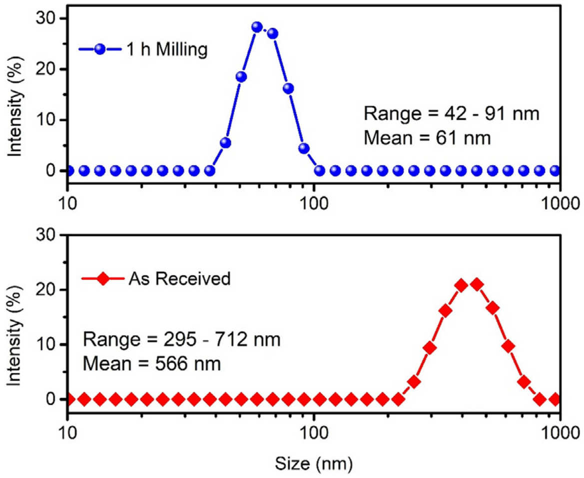

Fig. 3 – Dynamic Light Scattering (DLS) to measure the mean size of Nb_2O_5 particles as received and after milling.

Compositional analysis from EDS revealed the presence of carbon (Fig. 5B and Fig. 6B), oxygen (Fig. 5C and Fig. 6C) and

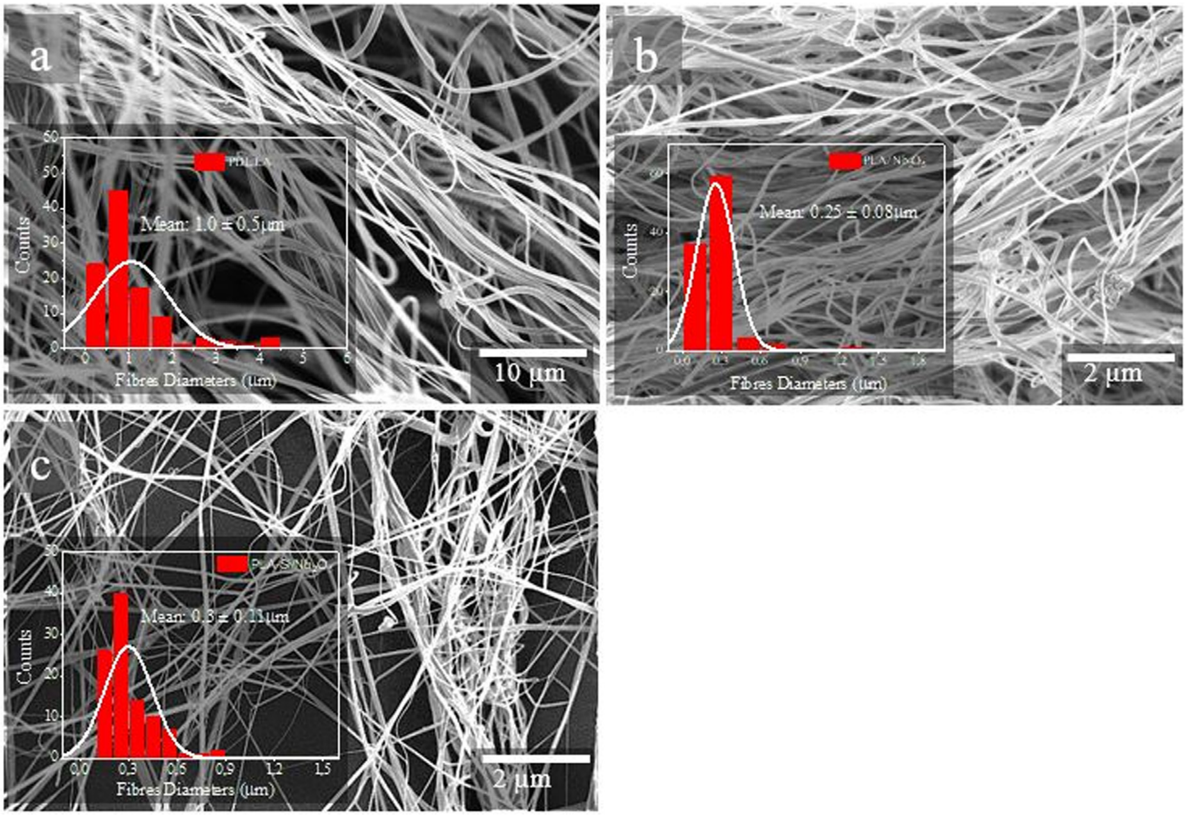

Fig. 4 – FESEM images of fibers morphology. (a) PDLLA images; (b) PDLLA-Nb_2O_5 and (c) PDLLA-SiO_2/Nb_2O_5. The mean of the fiber diameters presented 0.1 µm for the PDLLA; 0.2 µm for the PDLLA-Nb_2O_5 and 0.3 µm for the PDLLA + SiO_2/Nb_2O_5.

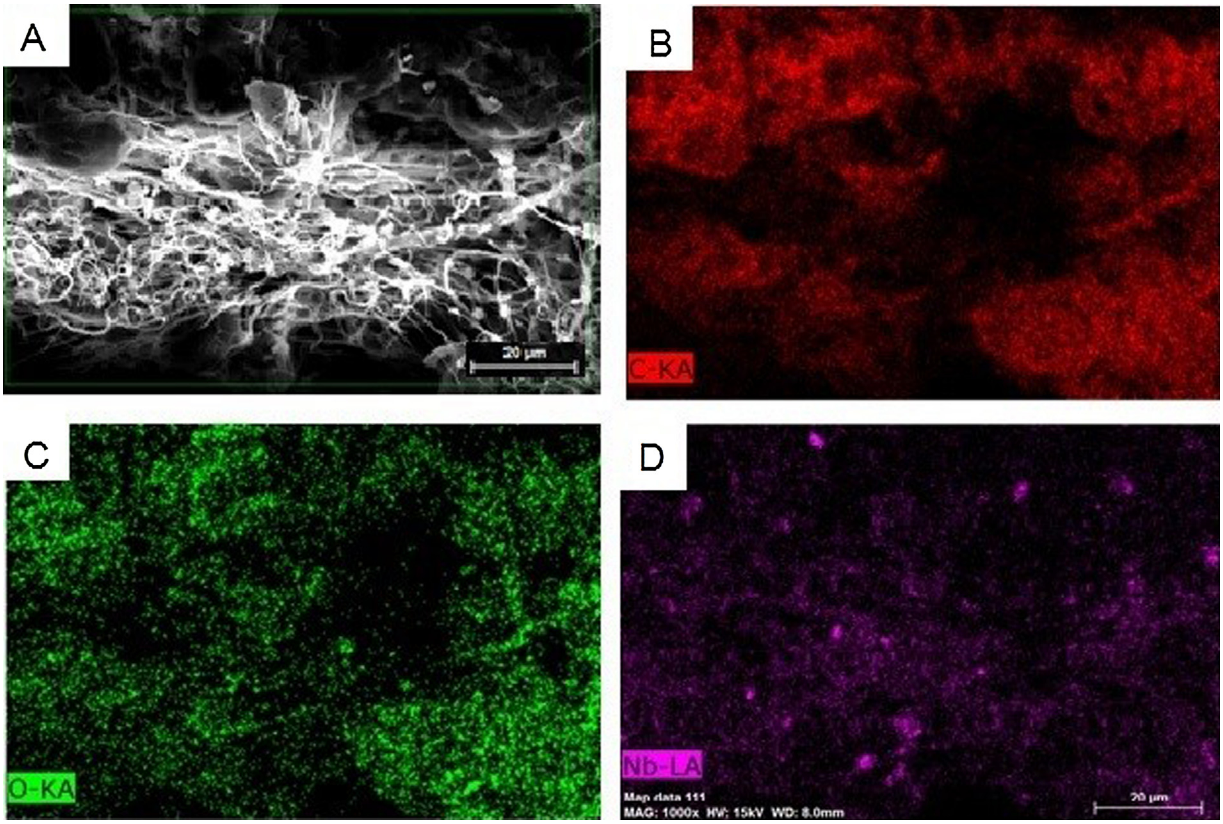

Fig. 5 – EDS mapping results on fibers. (A) fibers image, (B) carbon, (C) oxygen and (D) niobium.

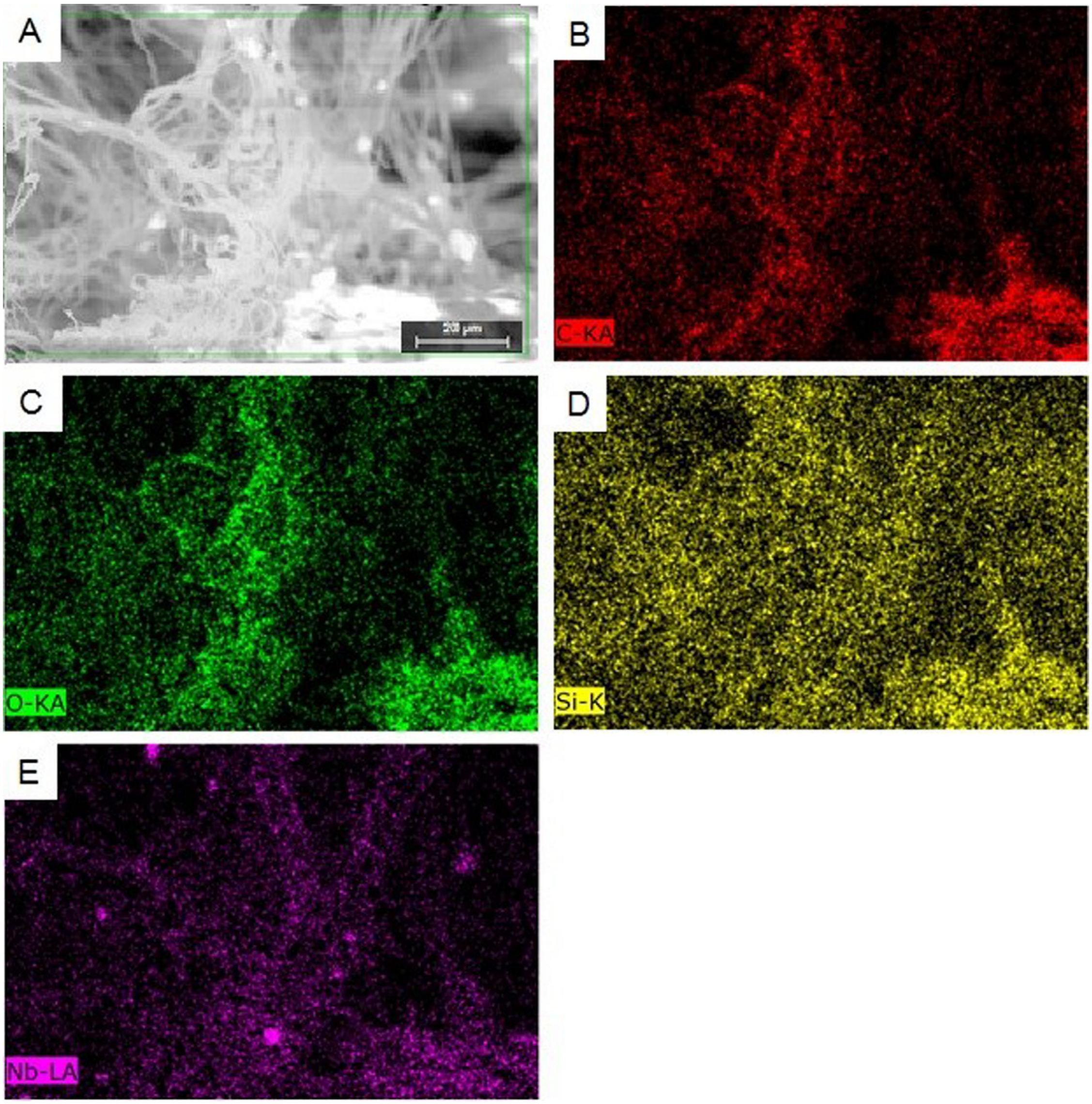

Fig. 6 – EDS mapping results on fibers. (A) fibers image, (B) carbon, (C) oxygen, (D) silicon and (E) niobium.

niobium (5D and 6E) in the Nb_2O_5-filled PDLLA fibers (Fig. 7). For the Nb_2O_5/SiO_2-filled PDLLA fiber, the silicon in the sol–gel samples was found as expected (Fig. 6D and Fig. 7).

The DSC curves (Fig. 8) showed that the inorganic content (Nb_2O_5 and SiO_2) does not significantly change the glass transition of the amorphous PDLLA fibers. These curves reported amorphous behavior of the fibers.

3.2. *Flexural strength and Knoop microhardness*

Overall, the incorporation of nanofibers into self-adhesive resin cement resulted in significant changes in flexural strength and microhardness. The additional of organic polymer itself (U200 + PDLLA fibers) did not differ from the control group (U200) without nanofiber (Table 1, $p > 0.05$). However, there was a significantly increase in the values of U200+Nb_2O_5-filled PDLLA composite fibers and U200+Nb_2O_5/SiO_2-filled PDLLA inorganic–organic hybrid fibers in comparison with

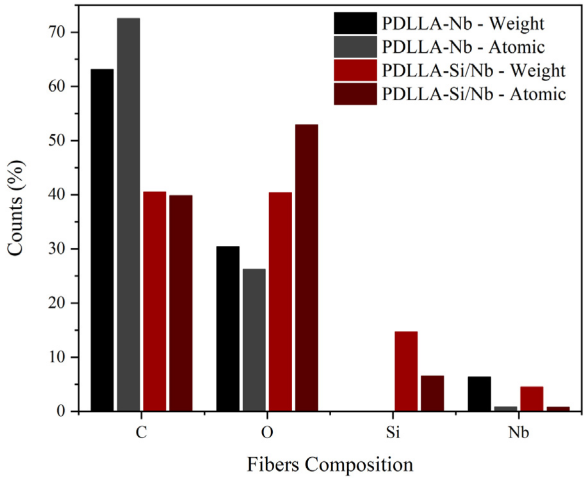

Fig. 7 – Element content in atomic percentage on the fibers developed.

Table 1 – Mean and standard deviation values of self-adhesive resin cement control and reinforced with nanofibers.

Groups	Flexural strength (MPa) (n = 5)	Hardness (KHN) (n = 6)	Degree of conversion (%) (n = 3)
(1) U200 (control)	42.3 ± 13.2^{a}	39.1 ± 0.8^{a}	67.6 ± 0.7^{b}
(2) U200 + PDLLA	57.5 ± 18.3^{ab}	45.8 ± 0.8^{ab}	61.5 ± 4.8^{ab}
(3) U200 + PDLLA/Ni_2O_5	71.0 ± 32.0^{b}	55.8 ± 1.9^{b}	63.2 ± 3.5^{ab}
(4) U200 + PDLLA/ Nb_2O_5/SiO_2	65.9 ± 6.3^{b}	60.7 ± 0.4^{b}	54.6 ± 4.9^{a}

Values in the same column with different superscript lower−case letters significantly differ from each other ($p < 0.05$).

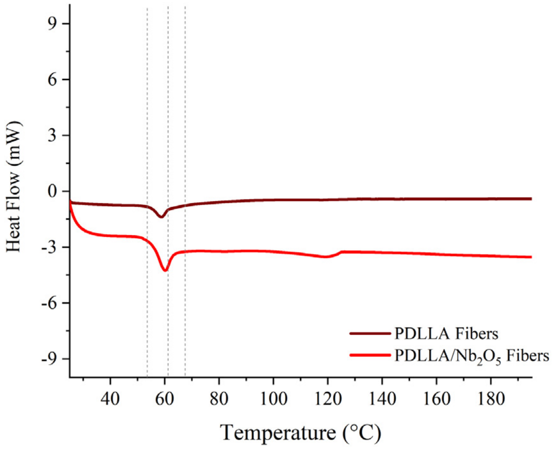

Fig. 8 – Differential Scanning Calorimetry (DSC) for characterization and stability analysis of niobium pentoxide into nanofibers.

U200 itself (Table 1, $p < 0.05$). The addition of fibers had an overall effect of increasing mechanical properties.

Although the addition of PDLLA fibers did not differ from the control group, there was no statistically difference among U200 + PDLLA, U200+Nb_2O_5-filled PDLLA and U200+Nb_2O_5/SiO_2-filled PDLLA ($p < 0.05$). However, the presence of U200+Nb_2O_5-filled PDLLA composite fibers and U200+Nb_2O_5/SiO_2-filled PDLLA inorganic–organic hybrid fibers showed higher values of hardness and flexural strength when compared to the control group ($p < 0.05$).

3.3. *Degree of conversion and SEM analyses*

For the DC test, the addition of PDLLA nanofibers and PDLLA-Ni_2O_5 into U200 did not differ from the negative control group (U200), $p < 0.05$. On the other hand, U200+ Nb_2O_5/SiO_2-filled PDLLA presented lower percentage values when compared to the other groups (Table 1).

SEM images showed that there was a good dispersion of nanofibers in the cement matrix (Fig. 9b). A good dispersion of nanofibers with the surrounding matrix without visible gaps (Fig. 9d) was also observed when compared to the unreinforced sample (Fig. 9c), but some artifacts are present in the samples without silica (Fig. 10b). These nanofibers remained intact after fracture as shown in Fig. 10a and d. Another pattern of fracture surface was observed in Fig. 10c with fibers pulling out of the matrix.

4. Discussion

The first part of this study focused on the synthesis and characterization of hybrid fibers that could be successfully incorporated into dental materials. Next, we evaluated the effect of their incorporation in a self-adhesive resin cement, and compared them to a self-adhesive resin cement without nanofibers (control) and a self-adhesive cement filled with organic nanofiber (PDLLA). Previous researches showed that reinforcement with organic polyacrylonitrile fibers resulted in improvements on the mechanical properties of composite resins [11,20,36]. In the current study, the PDLLA was chosen as organic phase because of its mechanical stability and biocompatibility [37]. However, the outcomes demonstrated that the addition of PDLLA nanofibers without Nb_2O_5 and Nb_2O_5/SiO_2 presented statistically similar values of flexural strength and hardness when compared with the self-adhesive resin cement itself (Table 1; $p > 0.05$). In contrast, the addition of hybrid nanofibers filled with Nb_2O_5 and Nb_2O_5/SiO_2 into the self-adhesive resin cement U200 notably presented high values of both flexure strength and hardness (Table 1, $p < 0.05$).

Mechanical resistance tests allow the prognosis of the clinical performance of luting agents with respect to the retentive strength of indirect restorations, because there is a correlation between the mechanical strength and the retentive strength of cemented prosthetic restorations [38]. Improvements in mechanical properties shown by present results could be explained by the physicochemical properties of Nb_2O_5 [17], such as high wear and corrosion resistance, which make it a stable material [17,39]. Mazur et al. [39] showed that a Nb_2O_5 layer deposited on a titanium alloy surface improved the SH of the alloy, which also makes Nb_2O_5 a potential coating that could prevent the deterioration of biomaterials by various environmental hazards.

Generally, when formulating self-adhesive resin cements, the fillers incorporated are composed of fluorosilicate glass, strontium calcium aluminosilicate glass, quartz, colloidal silica and other glass fillers [40]. As the acid-based reaction proceeds in the mixed cement, ionic cross-links that occur between acid groups and calcium ions or aluminum ions cause the pH to rise [40]. Madruga et al. [41] demonstrated that the addition of calcium hydroxide to self-adhesive resin cements reacted with the remaining acidic monomers and improved pH-neutralization, which in turn had significant impact on the mechanical stability of commercial self-adhesive cements [41,42]. The RelyX U200 used in the current study has calcium hydroxide in its composition, a compound that presents deficient mechanical properties and

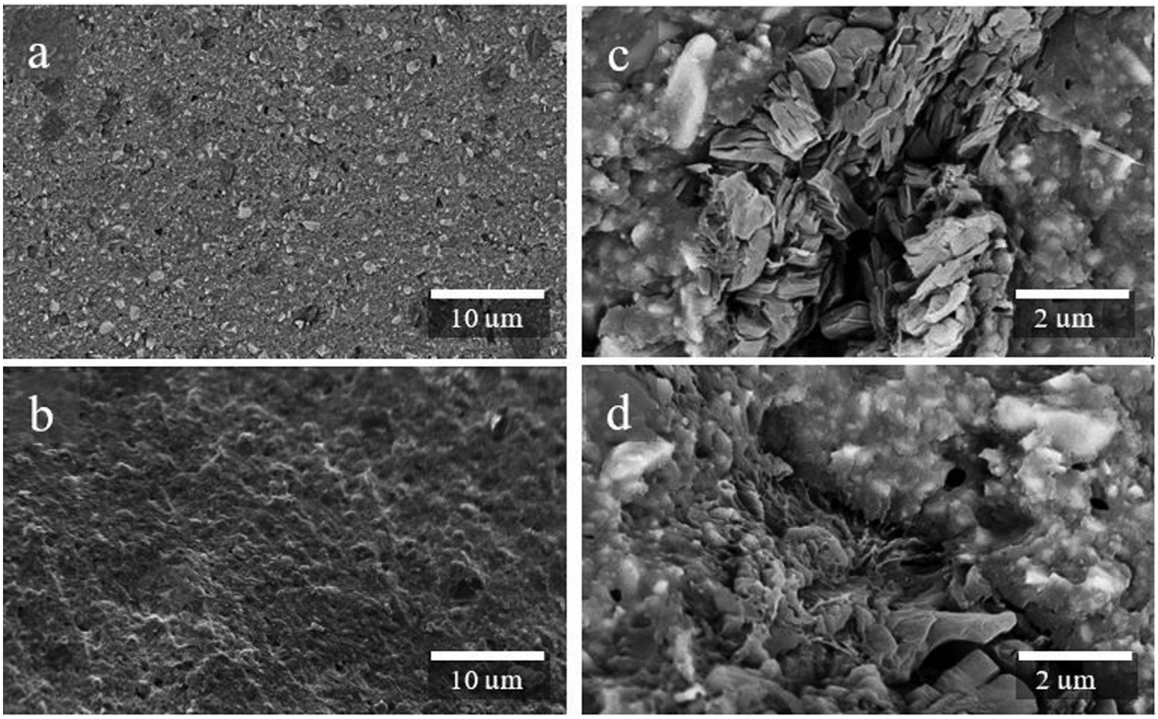

Fig. 9 – SEM images of fractured samples of (a) unreinforced resin cement: a smooth and planar fracture pattern is observed; (b) reinforced resin cement with PDLLA-Nb_2O_5-filled hybrid nanofiber: a rough surface characterizing the presence of nanofibers; (c) unreinforced resin cement presenting visible fillers and voids; (d) reinforced resin cement with PDLLA-Nb_2O_5-filled hybrid nanofiber. It is possible to note that even when the matrix around the nanofibers is broken, the cotton-wool like nanofibers still links the two layers they are inserted between.

may decrease the mechanical strength of resin-based materials [41,43]. As the results of the present study show, the addition of Nb_2O_5 in self-adhesive cements is appropriate to improve their mechanical properties. In addition, Nb_2O_5 neutralizes the pH of the polymerization kinetic reaction, as was shown when this oxide was added to bioglass [44]. The acidic functional monomers presented in self-adhesive cements require low pH and hydrophilic properties in the beginning of the setting reaction, but need further neutralizing reaction of the functional monomers to avoid impacting the end conversion of monomers and to reduce water sorption and solubility [40]. Such reaction could be boosted by the presence of Nb_2O_5 and improve the clinical performance of self-adhesive resin cements, but more studies are need in this area.

The improvement in the DC of resin-based materials is expected to increase wear resistance, fracture toughness and mechanical properties [45]. As Nb_2O_5 is a semiconductor oxide and presents high-energy absorption [18], higher DC values were expected in the samples with Nb_2O_5 and Nb_2O_5/SiO_2, because higher light absorption would improve the extent of the reaction of monomer into polymer. Moreover, Nb_2O_5 has band gap energy of 3.4 eV, presenting photocatalytic properties, which improves the light absorbtion near the visible wavelengths of the light spectrum [28]. This hypothesis was rejected, as no significant differences were found among the U200+ Nb_2O_5/SiO_2 compared with the U200 + PDLLA and U200 control ($p > 0.05$, Table 1), and a significant decrease occurred in DC for the U200+Nb_2O_5/SiO_2-filled PDLLA inorganic–organic hybrid nanofibers compared than in the other groups (Table 1, $p < 0.05$). The addition of fillers increases the viscosity of the resin cement, which may explain the decrease in the DC. Highly viscous cements present lower DC than low viscosity cements due to the reduced mobility of the monomers [46].

Habib et al. [47] demonstrated that smaller particles produced much higher depths of cure due to the decreased light scattering and reflection that is exhibited, particularly when matched with refractive index matched resins. The DC of light-cured materials depends on many factors, including the viscosity, filler characteristics and composition [5]. Since only U200+Nb_2O_5/SiO_2-filled PDLLA presented silica in the composition, its lower DC can be attributed to the presence of this compound in the nanofibers, which modifies the polymerization behavior, due to the refractive index difference which can influence the reflection and refraction effects that lead to turbidity or opacity [47]. It was also observed that PDLLA-Nb_2O_5/SiO_2 nanofibers presented higher diameters (300 nm) than the PDLLA-Nb_2O_5 (250 nm) (Fig. 4), which make light penetration difficult because the high content of filler or higher diameters obstruct the passage of light, thus resulting in a lower DC [48]. The processes led to the formation of fibers of wider diameters because they had incorporated the silica precursor.

The relationship between the DC and hardness is not always straightforward [49]. Although an increase in hardness is expected as the polymer network is formed, in the

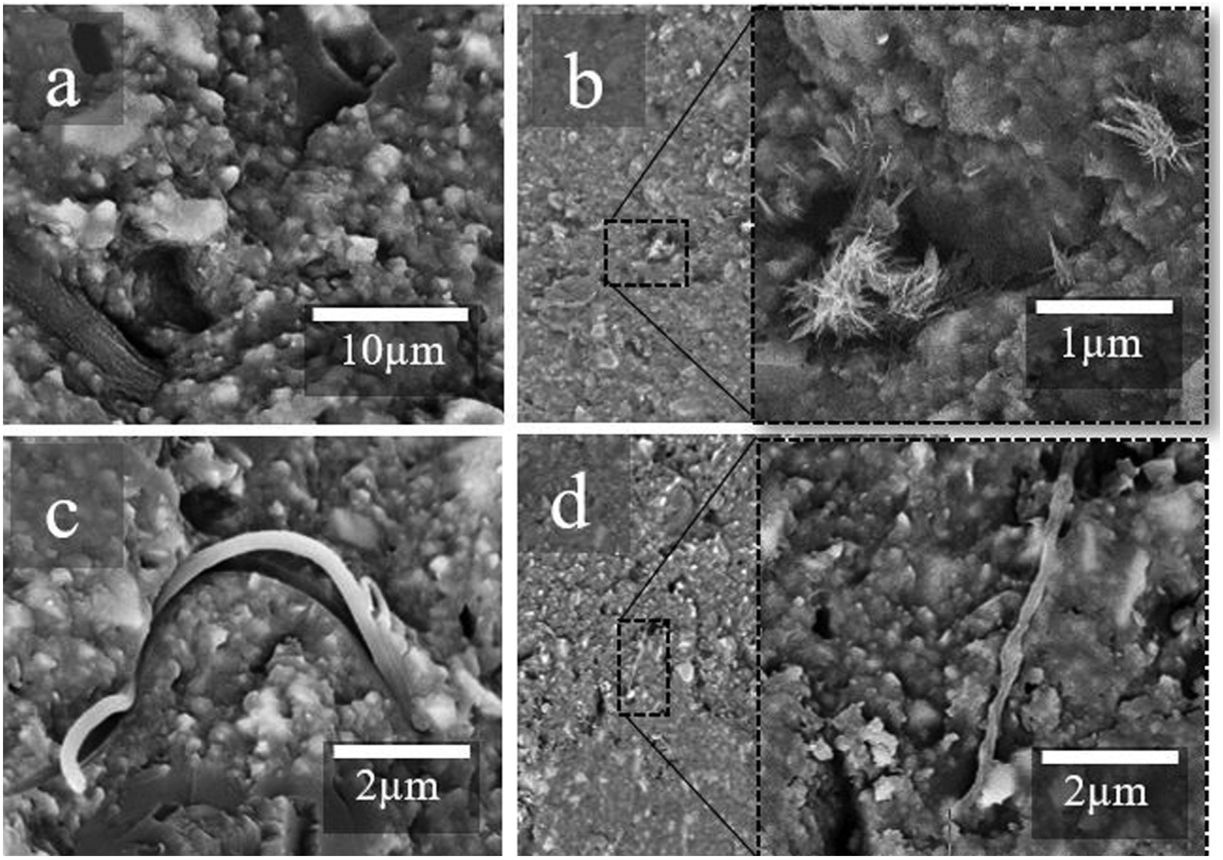

Fig. 10 – (a) Adhered nanofiber into the resin matrix (b) artifacts presented by cement without silica (c) pull-out pattern of the nanofibers from the resin matrix (d) cement and Nb_2O_5/SiO_2-filled PDLLA.

present study the addition of anisotropic fibers changed the hardness depending on the surface area and orientation of fibers. As shown in Table 1, no correlation between DC and hardness was found. While the addition of nanofibers had an overall effect of increasing mechanical properties, the DC showed an opposite trend. Despite such results, the minimum values for a clinically satisfactory restoration are not precise, although a range of 55–65% for DC is acceptable for resin-based materials and reached around 60% with resin cements [45,50]. The lower DC values presented by the U200+Nb_2O_5/SiO_2-filled PDLLA nanofibers did not affect their mechanical properties (Table 1) and is in accordance with those values previously reported in the literature [51].

Another aspect to be addressed when evaluating the DC is that in a two-paste dual-curing resin cement, obtaining the baseline spectrum of the FTIR is more difficult as the curing reaction begins immediately after mixing the pastes; whereas, the system is light-curable at any time during the chemical polymerization period [52]. To avoid this issue, spectra of base and catalyst pastes could be obtained separately and then averaged. However, a correlation has been shown between obtaining the spectra immediately after mixing the pastes and obtaining them separately [53]. In the present study, to consider a dual-cure condition, the analysis began immediately after mixing both pastes [18,41,54], inserted over the crystal and light-activated 3 min after mixing the pastes, by a single and calibrated operator.

According to some studies, dual-cure cements take up 6 min to photo activate because this delay has been shown to improve their mechanical properties, stimulating the chemical activation of the material [55,56]. However, this waiting time is clinically impracticable and it negates one of the main advantages presented by self-adhesive resin cements regarding their reducing chairside time. On the other hand, it was showed that a 4-minute interval between handling and photoactivation negatively impacted the DC [57]. This negative effect results from the chemical initiators starting the conversion that generates an increase in the viscosity of the material, preventing the photoactivation process from effectively participating in the conversion due to the advanced process of vitrification [58]. This vitrification process occurs during polymerization of resin cements and causes a rapid increase in the elasticity modulus of the material, which then becomes too rigid to allow free movement of the constituent components [57,58]. As our main objective was to evaluate the overall mechanical properties of a modified self-adhesive resin cement, the photo-activation was performed immediately after mixing and it was chosen to simulate a real clinical situation, because it is recommended that chemical-cured resin cements be applied soon after mixing and the restoration is seated [52].

When new materials are synthesized, it is important to set parameters to be evaluated. In this study, the DSC curves (Fig. 8) showed that the inorganic contents (Nb_2O_5 and SiO_2)

presented in hybrid fibers do not significantly change the glass transition of the amorphous PDLLA organic fibers. The glass transition temperature is an important property that determines the physical state of a polymer, and heating to temperatures above the glass transition the polymer may become elastic and rubber-like or liquefy [59], which is not the case. This is relevant data which allows the nanofibers to maintain their morphology during the light-curing processes. Therefore, along with their use in advanced applications for regeneration purposes such as bone and tissue scaffolds, drug delivery and catalyst enzyme carriers [23,24], hybrid nanofibers can be successfully used to reinforce self-adhesive resin cements, as shown herein.

The main advantage of using fiber materials instead of fillers as reinforcement in composites is their better load transfer ability due to the fiber bridging effects and the higher fracture aspect ratios [60]. A nanofibrous mat interleaved between two layers of a laminate can bridge the two plies even when the matrix is broken, carrying on additional loads [61]. In the present study, SEM images of the fractured surfaces of unreinforced samples (Fig. 9a and c) and reinforced ones (Fig. 9b and d) are shown. The surface of the unreinforced cement was smooth, planar and had relatively large fracture steps or voids (Fig. 9a), indicating low resistance to the applied force during breaking. The fractured surfaces of the reinforced cement were rough (Fig. 9b). According to Tian et al. [20], a rough surface suggests the presence of nanofibers effectively deflected crack propagation. The rougher surface (Fig. 9b) suggests energy consumption during fracture, and consequently, enhanced fracture resistance [62]. Indeed, we observed that even though the sample had been fractured, the nanofibers remained intact as observed in Fig. 10, a fact also responsible for minimizing the dispersion of tension and increasing the strength of the material [56]. Even when the matrix around the nanofibers (Fig. 9d) is broken, the cotton-wool-like nanofibers still link the two layers between which they are inserted, which does not occur in the sample without nanofibers (Fig. 9c), providing good load transfer between them, which ensures that the load is transferred to the stronger fiber and this is how the fiber actually works as a reinforcement [61,63].

No attempts were made to chemically pre-treat the nanofibers. They were packed during the process and presented an adequate wetting, which supported the positive interaction of the fibers with the matrix [11]. However, when the sol–gel method was used to produce the inorganic–organic hybrid fibers with a silica precursor, a wet-chemical process occurred to functionalize the inorganic particles during the process with the PDLLA, turning it to organofunctional. The chemistry of the sol–gel process is based on hydrolysis and polycondensation reactions resulting in the linking of organic and inorganic sol–gel materials by stable chemical bonds [64]. It has been shown that a strong interaction between the niobium and silica oxides is established during the sol–gel process, i.e., it involves the formation of Si—O—Nb bonds. The Nb—O—Si linkages on the surface were found by the spectra of approximately 850 cm^{-1} (Fig. 2) formed during the process, giving rise to the higher structural stability of the SiO_2–Nb_2O_5 system [65]. This explains the enhanced adhesion and dispersion of the PDLLA + Ni_2O_5/SiO_2 into the U200 shown by Fig. 10d compared with 10b (U200+ PDLLA-Ni_2O_5), which presented some artifacts on the surface, although it did not influence the overall results of the mechanical properties. In the EDS mapping (Figs. 5D and 6E), it was observed that niobium did not agglomerate within the surface of the nanofibers and it is important to enhance the interaction between the fibers' surface and the resin cement.

Fig. 10c shows that the fracture surfaces in fiber-containing composites also present other fracture patterns with fibers pulling out of the matrix. Such fracture patterns occur when the distance between the matrix crack and the end of the fiber is less than the critical length and the fibers do not fracture within the matrix. It implies that frictional and interlocking resistance occurred and resulted in more energy consumption for the fracture to happen [66], as previously observed in other studies with fibers or whiskers in dental composites [11,67]. The effect of fiber pull-out provides extra toughening mechanisms since the pulled-out fibers also assist in bridging the cracks [21]. The diameter of the fibers plays an important role in the mechanical properties of composite resin materials [13], since nanofibers of lower diameters are more ductile (average failure strain stayed over 50%) and tougher [22]. Although nanofibers can be synthetized by different techniques and electro-spinning is the widely adopted method, it suffers several drawbacks, such as the requirement for specialized equipment, high electrical potential, and electrically conductive targets [68]. The SBS expanded the market to overcome such restrictions of the conventional electrospinning technique and was able to fabricate non-woven webs of fibers with diameters in the same size scale as those produced during electro-spinning in a rapid way [69].

This is a first exploratory study aiming to understand the series of events relating to the incorporation of hybrid nanofibers in dental materials. Some limitations of the present study are highlighted: (1) we evaluated only the immediate DC after mixing the base and catalyst pastes but further studies with this modified self-adhesive resin cement are important to compare the DC at different times upon irradiance, since the addition of Nb_2O_5 could neutralize the pH of the polymerization kinect reaction, as previously showed when this oxide was added to bioglass [44]; (2) Although this research focuses on self-adhesive cements as they have lower mechanical properties than conventional resin cements [70], a commercial material was used and, consequently, it is not possible to fully compare the different categories of the materials as they differ in the organic matrixes and inorganic compounds. Considering the promising results we present, and with the knowledge that hybrid nanofibers have been successfully processed and offer a promising reinforcement alternative to organic fibers or fillers, the present outcomes encourage more research with hybrid nanofibers in the field of dental materials.

Overall, we highlight that incorporating hybrid composite and inorganic–organic fibers into a self-adhesive resin cement has shown to be a promising approach to improve the mechanical properties of dental materials. In addition, hybrid nanofibers can be embedded using different oxides and therapeutic ions, presenting both mechanical and bioactive improvements. The addition of nanofibers incorporating Nb_2O_5 powder with and without sol–gel silica increased the mechanical properties of the resin cement. Owing to the knowledge that niobium oxide promotes crystal growth and biomimetic mineralization of adjacent tissues, further studies will address it to extend the applications of resin cements in clinical practice.

5. Conclusions

The incorporation of 1 wt.% inorganic–organic hybrid fibers embedded with niobium pentoxide provided the highest mechanical properties among all materials tested, which makes them a potential reinforcing agent for resin cements and dental materials.

Acknowledgments

This study was financed by the Coordenação de Aperfeiçoamento de Pessoal de Nível Superior - Brazil (CAPES) - Finance Code 001 as part of the post-doctoral research of the first author. It was also supported from CNPq (Brazil) Grant number PVE 304898/2014-7 and CAPES-PDSE88881.132372/2016-01. We thank FAPESP (#grant 2019/06045-2) and also thank AMG Brasil for donating niobium oxide powders. The authors wish to thank Prof. Rubens M. do Nascimento (UFRN) for FESEM analysis.

REFERENCES

[1] el-Mowafy O. The use of resin cements in restorative dentistry to overcome retention problems. J Can Dent Assoc 2001;67(2):97–102.
[2] Radovic I, Monticelli F, Goracci C, Vulicevic ZR, Ferrari M. Self-adhesive resin cements: a literature review. J Adhes Dent 2008;10(4):251–8.
[3] Habekost Lde V, Camacho GB, Demarco FF, Powers JM. Tensile bond strength and flexural modulus of resin cements-influence on the fracture resistance of teeth restored with ceramic inlays. Oper Dent 2007;32(5):488–9.
[4] De Munck J, Vargas M, Van Landuyt K, Hikita K, et al. Bonding of an auto-adhesive luting material to enamel and dentin. Dent Mater 2004;20(10):963–71.
[5] Vrochari AD, Eliades G, Hellwig E, Wrbas KT. Curing efficiency of four self-etching, self-adhesive resin cements. Dent Mater 2009;25(9):1104–8.
[6] Pisani-Proença J, Erhardt MC, Amaral R, Valandro LF, Bottino MA, et al. Influence of different surface conditioning protocols on microtensile bond strength of self-adhesive resin cements to dentin. J Prosthet Dent 2011;105(4):227–35.
[7] Santos MJ, Bapoo H, Rizkalla AS, Santos GC. Effect of dentin-cleaning techniques on the shear bond strength of self-adhesive resin luting cement to dentin. Oper Dent 2011;36(5):512–20.
[8] Arrais CA, Giannini M, Rueggeberg FA. Kinetic analysis of monomer conversion in auto- and dual-polymerizing modes of commercial resin luting cements. J Prosthet Dent 2009;101(2):128–36.
[9] Tezvergil-Mutluay A, Lassila LV, Vallittu PK. Degree of conversion of dual-cure luting resins light-polymerized through various materials. Acta Odontol Scand 2007;65(4):201–5.
[10] Wang R, Zhang M, Liu F, Bao S, Wu T, Jiang X, et al. Investigation on the physical-mechanical properties of dental resin composites reinforced with novel bimodal silica nanostructures. Mater Sci Eng C Mater Biol Appl 2015;50:266–73.
[11] Vidotti HA, Manso AP, Leung V, do Valle AL, Ko F, Carvalho RM. Flexural properties of experimental nanofiber reinforced composite are affected by resin composition and nanofiber/resin ratio. Dent Mater 2015;31(9):1132–41.
[12] Chiari MD, Rodrigues MC, Xavier TA, de Souza EM, Arana-Chavez VE, Braga RR. Mechanical properties and ion release from bioactive restorative composites containing glass fillers and calcium phosphate nano-structured particles. Dent Mater 2015;31(6):726–33.
[13] Leitune VC, Collares FM, Trommer RM, Andrioli DG, Bergmann CP, Samuel SM. The addition of nanostructured hydroxyapatite to an experimental adhesive resin. J Dent 2013;41(4):321–7.
[14] Elsaka SE, Hamouda IM, Swain MV. Titanium dioxide nanoparticles addition to a conventional glass-ionomer restorative: influence on physical and antibacterial properties. J Dent 2011;39(9):589–98.
[15] D'Alpino PH, Silva MS, Vismara MV, Di Hipólito V, Miranda González AH, et al. The effect of polymerization mode on monomer conversion, free radical entrapment, and interaction with hydroxyapatite of commercial self-adhesive cements. J Mech Behav Biomed Mater 2015;46:83–92.
[16] Ramos-Tonello CM, Lisboa-Filho PN, Arruda LB, Tokuhara CK, Oliveira RC, et al. Titanium dioxide nanotubes addition to self-adhesive resin cement: effect on physical and biological properties. Dent Mater 2017;33(7):866–75.
[17] Balbinot GS, Collares FM, Visioli F, Soares PBF, Takimi AS, Samuel SMW, et al. Niobium addition to sol–gel derived bioactive glass powders and scaffolds: in vitro characterization and effect on pre-osteoblastic cell behavior. Dent Mater 2018;34(10):1449–58.
[18] Shan Y, Zheng Z, Liu J, Yang Y, Li Z, Huang Z, et al. Niobium pentoxide: a promising surface-enhanced Raman scattering active semiconductor substrate. Comput Mater 2017;3: 11.
[19] Karlinsey RL, Hara AT, Yi K, et al. Bioactivity of novel self-assembled crystalline Nb2O5 microstructures in simulated and human saliva. Biomed Mater 2006;1:16–23.
[20] Tian M, Gao Y, Liu Y, Liao Y, Xu R, Hedin NE, et al. Bis-GMA/TEGDMA dental composites reinforced with electrospun nylon 6 nanocomposite nanofibers containing highly aligned fibrillar silicate single crystals. Polymer (Guildf) 2007;48(9):2720–8.
[21] Wang X, Cai Q, Zhang X, Wei Y, Xu M, Yang X, et al. Improved performance of Bis-GMA/TEGDMA dental composites by net-like structures formed from SiO2 nanofiber fillers. Mater Sci Eng C Mater Biol Appl 2016;59:464–70.
[22] Papkov D, Zou Y, Andalib MN, Goponenko A, Cheng SZ, Dzenis YA. Simultaneously strong and tough ultrafine continuous nanofibers. ACS Nano 2013;7(4):3324–31.
[23] Jones JR. Review of bioactive glass: from Hench to hybrids. Acta Biomater 2013;9:4457–86, http://dx.doi.org/10.1016/j.actbio.2012.08.023.
[24] Zhou P, Wang J, Maçon ALB, Obata A, Jones JR, Kasuga T. Tailoring the delivery of therapeutic ions from bioactive scaffolds while inhibiting their apatite nucleation: a coaxial electrospinning strategy for soft tissue regeneration. RSC Adv 2017;7:3992–9, http://dx.doi.org/10.1039/C6RA25645G.
[25] Tallia F, Russo L, Li S, Orrin ALH, Shi X, Chen S, et al. Bouncing and 3D printable hybrids with self-healing properties. Mater Horizons 2018;5:849–60, http://dx.doi.org/10.1039/c8mh00027a.
[26] Sun W, Cai Q, Li P, Deng X, Wei Y, Xu M, et al. Post-draw PAN-PMMA nanofiber reinforced and toughened Bis-GMA dental restorative composite. Dent Mater 2010;26(9): 873–80.

[27] Hoppe A, Mouriño V, Boccaccini AR. Therapeutic inorganic ions in bioactive glasses to enhance bone formation and beyond. Biomater Sci 2013;1:254–6, http://dx.doi.org/10.1039/C2BM00116K.

[28] Prado AGS, Jurandir EAF, de Jocilene RS, Torres D. Ammonium complex of niobium as a precursor for the hydrothermal preparation of cellulose acetate/Nb_2O_5 photocatalyst. J Mol Catal A Chem 2005;2:115–9.

[29] Rodrigues RF, Ramos CM, Francisconi PA, Borges AF. The shear bond strength of self-adhesive resin cements to dentin and enamel: an in vitro study. J Prosthet Dent 2015;113(3):220–7.

[30] Simões TC, Luque-Martinez Í, Moraes RR, Sá A, Loguercio AD, et al. Longevity of bonding of self-adhesive resin cement to dentin. Oper Dent 2016;41(3):E64–72.

[31] Poologasundarampillai G, Yu B, Jones JR, Kasuga T. Electrospun silica/PLLA hybrid materials for skeletal regeneration. Soft Matter 2011;7:10241, http://dx.doi.org/10.1039/c1sm06171b.

[32] Medeiros ELG, Braz AL, Porto IJ, Menner A, Bismarck A, Boccaccini AR, et al. Porous bioactive nanofibers via cryogenic solution blow spinning and their formation into 3D macroporous scaffolds. ACS Biomater Sci Eng 2016;2:1442–9, http://dx.doi.org/10.1021/acsbiomaterials.6b00072.

[33] Alwattar A, Haddad A, Zhou Q, Nascimento T, Greenhalgh R, Medeiros E, et al. Synthesis and characterisation of fluorescent pyrene end capped polylactide fibers. Polym Int 2018, http://dx.doi.org/10.1002/pi.5712.

[34] Magaz A, Roberts AD, Faraji S, Nascimento TRL, Medeiros ES, Zhang W, et al. Porous, aligned and biomimetic fibers of regenerated silk fibroin produced by solution blow spinning. Biomacromolecules 2018, http://dx.doi.org/10.1021/acs.biomac.8b01233.

[35] Andreatta LML, Furuse AY, Prakki A, Bombonatti JF, Mondelli RF. Pulp chamber heating: an in vitro study evaluating different light sources and resin composite layers. Braz Dent J 2016;27(6):675–80.

[36] Fong H. Electrospun nylon6 nanofiber reinforced Bis-GMA/TEGDMA dental restorative composite resins. Polymer 2004;45:2427–32.

[37] Hamad K, Kaseem M, Ko YG, Deri F. Biodegradable polymer blends and composites: an overview. Polym Sci Ser A 2014;56:812–29.

[38] Grieve AR. A study of dental cements. Br Dent Nurs J 1969;127(4):405–10.

[39] Mazur M, Kalisz M, Wojcieszak D, Grobelny M, Mazur P, Kaczmarek D, et al. Determination of structural, mechanical and corrosion properties of Nb2O5 and (NbyCu 1-y)Ox thin films deposited on Ti6Al4V alloy substrates for dental implant applications. Mater Sci Eng C Mater Biol Appl 2015;47:211–21.

[40] Ferracane JL, Stansbury JW, Burke FJ. Self-adhesive resin cements - chemistry, properties and clinical considerations. J Oral Rehabil 2011;38(4):295–314.

[41] Madruga FC, Ogliari FA, Ramos TS, Bueno M, Moraes RR. Calcium hydroxide, pH-neutralization and formulation of model self-adhesive resin cements. Dent Mater 2013;29(4):413–8.

[42] Zorzin J, Petschelt A, Ebert J, Lohbauer U. pH neutralization and influence on mechanical strength in self-adhesive resin luting agents. Dent Mater 2012;28:672–9.

[43] Niinuma A. Newly developed resinous direct pulp capping agent containing calcium hydroxide (MTYA1-Ca). Int Endod J 1999;32:475–83.

[44] Lopes JH, Magalhães A, Mazali IO, et al. Effect of niobium oxide on the structure and properties of melt-derived bioactive glasses. J Am Chem Soc 2014;97:3843–52.

[45] Ferracane JL, Mitchem JC, Condon JR, Todd T. Wear and marginal breakdown of composites with various degree of cure. J Dent Res 1997;76(8):1508–16.

[46] Di Francescantonio M, Aguiar TR, Arrais CA, Cavalcanti AN, Davanzo CU, et al. Influence of viscosity and curing mode on degree of conversion of dual-cured resin cements. Eur J Dent 2013;7(1):81–5.

[47] Habib E, Wang R, Zhu XX. Monodisperse silica-filled composite restoratives mechanical and light transmission properties. Dent Mater 2017;33(3):280–7.

[48] Altmann ASP, Collares FM, Balbinot GS, Leitune VCB, Takimi AS, Samuel SMW. Niobium pentoxide phosphate invert glass as a mineralizing agent in an experimental orthodontic adhesive. Angle Orthod 2017;87(5):759–65.

[49] Furuse AY, Mondelli J, Watts DC. Network structures of Bis-GMA/TEGDMA resins differ in DC, shrinkage-strain, hardness and optical properties as a function of reducing agent. Dent Mater 2011;27(5):497–506.

[50] Kumbuloglu O, Lassila LV, User A, Vallittu PK. A study of the physical and chemical properties of four resin composite luting cements. Int J Prosthodont 2004;17(3):357–63.

[51] Rizzante FAP, Locatelli PM, Porto TS, Borges AFS, Mondelli RFL, Ishikiriama SK. Physico-mechanical properties of resin cement light cured through different ceramic spacers. J Mech Behav Biomed Mater 2018;85:170–4.

[52] Yan YL, Kim YK, Kim KH, Kwon TY. Changes in degree of conversion and microhardness of dental resin cements. Oper Dent 2010;35(2):203–10.

[53] Calgaro PA, Furuse AY, Correr GM, Ornaghi BP, Gonzaga CC. Influence of the interposition of ceramic spacers on the degree of conversion and the hardness of resin cements. Braz Oral Res 2013;27(5):403–9.

[54] Augusto CR, Leitune VCB, Ogliari FA, Collares FM. Influence of an iodonium salt on the properties of dual-polymerizing self-adhesive resin cements. J Prosthet Dent 2017;118(2):228–34.

[55] Furuse AY, Santana LOC, Rizzante FAP, Ishikiriama SK, Bombonatti JF, Correr GM, et al. Delayed light activation improves color stability of dual-cured resin cements. J Prosthodont 2018;27(5):449–55.

[56] Soares CJ, Bicalho AA, Verissimo C, Soares P, Tantbirojn D, Versluis A. Delayed photo-activation effects on mechanical properties of dual cured resin cements and finite element analysis of shrinkage stresses in teeth restored with ceramic inlays. Oper Dent 2016;41(5):491–500.

[57] da Silva Fonseca AS, Mizrahi J, Menezes LR, Valente LL, de Moraes RR, et al. The effect of time between handling and photoactivation on self-adhesive resin cement properties. J Prosthodont 2014;23(4):302–7.

[58] Chen HY, Manhart J, Hickel R, Kunzelmann KH. Polymerization contraction stress in light-cured packable composite resins. Dent Mater 2001;17(3):253–9.

[59] Boyer RF. Encyclopedia of polymer science and technology. New York: Wiley Interscience; 1977.

[60] Chen L, Yu Q, Wang Y, Li H. BisGMA/TEGDMA dental composite containing high aspect-ratio hydroxyapatite nanofibers. Dent Mater 2011;27(11):1187–95.

[61] Palazzetti R, Zucchelli A, Trendafilova I. The selfreinforcing effect of nylon 6,6 nano-fibres on CFRP laminates subjected to low velocity impact. Compos Struct 2013;106:661–71.

[62] Borges ALS, Münchow EA, de Oliveira Souza AC, Yoshida T, Vallittu PK, Bottino MC. Effect of random/aligned nylon-6/MWCNT fibers on dental resin composite reinforcement. J Mech Behav Biomed Mater 2015;48: 134–44.

[63] Arcos D, Vallet-Regí M. Sol-gel silica-based biomaterials and bone tissue regeneration. Acta Biomater 2010;6(8): 2874–88.

[64] Schubert U, Husing N, Lorenz A. Hybrid inorganic -organic materials by sol-gel processing of organofunctional metal alkoxides. Chem Material 1995;7:2010–27.

[65] Francisco MSP, Gushikem Y. Synthesis and characterization of SiO_2–Nb_2O_5 systems prepared by the sol–gel method: structural stability studies. J Mater Chem 2002;12:2552–8, http://dx.doi.org/10.1039/B200685E.

[66] Quinn GD. Guide to practice for fractography of ceramics and glasses. SP: NIST special publication; 2007. p. 960–1016.

[67] Zhang H, Darvell BW. Mechanical properties of hydroxyapatite whisker-reinforced bis-GMA-based resin composites. Dent Mater 2012;28:824–30.

[68] Behrens AM, Casey BJ, Sikorski MJ, Wu KL, Tutak W, Sandler AD, et al. In situ deposition of PLGA nanofibers via solution blow spinning. ACS Macro Lett 2014;3:249–54.

[69] Medeiros ES, Glenn GM, Klamczynski AP, Orts WJ, Mattoso LHC. Solution blow spinning : a new method to produce micro- and nanofibers from polymer solutions. J Appl Polym Sci 2009;113(4):2322–30.

[70] Furuichi T, Takamizawa T, Tsujimoto A, Miyazaki M, Barkmeier WW, Latta MA. Mechanical properties and sliding-impact wear resistance of self-adhesive resin cements. Oper Dent 2016;41(3):E83–92.